

Raman Spectroscopic Studies of Temperature Dependent Anomalies of Strontium, Barium, Lead, and Calcium Nitrate

M. H. BROOKER

Chemistry Department, Memorial University of Newfoundland, St. John's, Newfoundland, Canada

Received May 5, 1978; in revised form July 15, 1978

Raman studies of normal and ^{18}O -substituted $\text{Sr}(\text{NO}_3)_2$ have been performed over a range of temperatures (77 to 580°K) to investigate the anomalous component previously observed in the symmetric stretching region. The results suggest that the peak may have a hot band origin. Impurity ions, $\text{N}^{18}\text{O}^{16}\text{O}_2^-$ and vibrationally excited $^*\text{NO}_3^-$ ions, give rise to local modes (deep-well impurity centers) in the ν_1 and ν_4 ($\text{N}^{18}\text{O}^{16}\text{O}_2^-$ only) regions but delocalized modes (shallow-well impurity centers) in the other internal and external mode regions. The host lattice was able to tolerate a large fraction of this type of impurity without interference with the dynamical coupling. Anomalous properties previously reported appear to be due to freezing out of the hot band. A less complete study of $\text{Ca}(\text{NO}_3)_2$, $\text{Ba}(\text{NO}_3)_2$ and $\text{Pb}(\text{NO}_3)_2$ at room temperature and at temperature near 500°K suggests behavior similar to $\text{Sr}(\text{NO}_3)_2$.

Introduction

The correct assignment of space group symmetries to chemically simple crystals is not always a trivial problem. Considerable effort has been expended attempting to deduce whether the structures of $\text{Sr}(\text{NO}_3)_2$, $\text{Ba}(\text{NO}_3)_2$, $\text{Ca}(\text{NO}_3)_2$ and $\text{Pb}(\text{NO}_3)_2$ are centrosymmetric (1-6). Two structures have been proposed, the centric structure $\text{Pa}3(T_h^6)$ and the non-centric $P2_13(T^4)$. Early X-ray data were analyzed to give the $\text{Pa}3$ structure but Birnstock (2) detected a number of weak forbidden reflections for $\text{Ba}(\text{NO}_3)_2$ and concluded that the non-centric $P2_13$ structure was correct. Although Birnstock's use of an isotopic temperature factor may not be valid his conclusions have gained some support as a result of the detection of several other anomalous properties (3-5). Previously (1) we reported a detailed infrared and Raman study of these crystals and concluded that the vibrational spectro-

scopic evidence supported the $\text{Pa}3$ structure. The conclusions were based on the excellent agreement between the spectroscopic data and the predictions based on unit-cell group analysis and the failure to detect the presence of "two-site" splitting or Raman activity of the longitudinal optic mode (both required by the $P2_13$ structure).

Obviously the difference between the two structures must be small and one wonders what degree of imperfection can be tolerated before the $\text{Pa}3$ structure shows signs of lower symmetry. Packing faults, substitutional defects (other cations and anions) and occluded water are estimated to be present in these crystals to less than 1% and although important for some measurements are not likely to significantly affect the vibrational spectrum. In the present study we have attempted to deduce the effect of impurities through measurements of both vibrationally excited, and oxygen-18 substituted nitrate groups. Recent studies (7-11) have shown

that most ionic nitrates contain a significant number of nitrate groups that are disordered with respect to the ordered lattice and that these groups may result from the thermal population of upper vibrational states with associated anharmonicity. Anharmonic effects can also lead to the presence of normally forbidden Bragg peaks (12) so it seems possible that the anomalous X-ray and spectroscopic results have a similar origin.

Experimental

All samples were prepared from reagent grade salts which had been dissolved in water, treated with activated charcoal (to remove fluorescent impurities) filtered through a fine frit and recrystallized by slow evaporation. An 8% ^{18}O -enriched sample of $\text{Sr}(\text{NO}_3)_2$ was prepared from the reaction of $\text{Sr}(\text{NO}_3)_2$ and HNO_3 with 50% ^{18}O -enriched water followed by evaporation to the solid. A small single crystal of 8% ^{18}O - $\text{Sr}(\text{NO}_3)_2$ was grown by slow evaporation of a solution in a capillary tube. Isotopic composition was determined from the integrated Raman intensities of the symmetric stretching modes of the isotopic ions (13). The peak position and percent abundance for each species were: $\text{N}^{16}\text{O}_3^-$, 1056 cm^{-1} , 80%; $\text{N}^{18}\text{O}^{16}\text{O}_2^-$, 1046 cm^{-1} , 17%; $\text{N}^{18}\text{O}_2^{16}\text{O}^-$, 1016 cm^{-1} , 3.5%; $\text{N}^{18}\text{O}_3^-$, 996 cm^{-1} , $\sim 0.05\%$; $\text{N}^{17}\text{O}^{16}\text{O}_2^-$, 1046 cm^{-1} , 0.6%. This works out to an overall 8.0% ^{18}O enrichment. The $\text{N}^{18}\text{O}_2^{16}\text{O}^-$, $\text{N}^{18}\text{O}_3^-$ and $\text{N}^{17}\text{O}^{16}\text{O}_2^-$ species were not studied in detail because of their low intensities.

Raman spectra were obtained for all samples as dry powders. The 8.0% ^{18}O - $\text{Sr}(\text{NO}_3)_2$ was measured at selected temperatures from 77 to 580°K while $\text{Ca}(\text{NO}_3)_2$, $\text{Ba}(\text{NO}_3)_2$ and $\text{Pb}(\text{NO}_3)_2$ were measured at room temperature and at a temperature about 500°K. The room temperature data were essentially identical to a previous report (1). Raman spectra were also obtained for the 8.0% ^{18}O -enriched

crystal of $\text{Sr}(\text{NO}_3)_2$ at 77, 298 and 478°K. A clear well-formed single crystal of $\text{Sr}(\text{NO}_3)_2$ was used to investigate the external mode region over the temperature range 77 to 450°K. Both incident and scattered light were paralleled to principle axes and depolarization ratios of about 0.05 were obtained for A_{1g} modes.

Raman spectra were measured with a Coderg PHO Raman spectrometer after sample excitation with the 488.0 nm line of a Control Laser, model 553A argon ion laser. Plasma lines from the laser were removed with a narrow band-pass interference filter. Peak positions were calibrated against laser plasma lines at 1044.0 and 1057.3 cm^{-1} and are probably accurate to $\pm 0.2\text{ cm}^{-1}$. Power levels at the samples were approximately 500 mw. Polarization of the incident beam was controlled by a half-wave plate, and the 90° scattered light was analyzed with Polaroid film placed before the monochromator slit. Room temperature spectra (298°K) were recorded from samples placed on a constant temperature copper block. The 77°K temperature was achieved with a liquid nitrogen evaporating cryostat while high temperature spectra were obtained for samples sealed in glass tubing and placed in an insulated furnace. Temperatures were monitored with a chromel-alumel thermocouple in contact with the glass tubing. Sample temperatures were constant to $\pm 3^\circ$ but it is possible that sample temperatures at the laser focus were somewhat higher than the thermocouple reading.

To aid in the contour analysis of the symmetric stretching modes the photon counting output was interfaced to a PDP 11/40 computer and the counts collected digitally at 0.125 cm^{-1} intervals. The photon counts were smoothed with a 9 point smoothing function, corrected for baseline and curve resolved. The symmetric stretching mode of the $\text{N}^{18}\text{O}^{16}\text{O}_2^-$ ion (and the $\text{N}^{16}\text{O}_3^-$ ion at high temperature) appeared as a strong sharp peak ("a" component) with a low frequency

shoulder (the anomalous "b" component). Peak maxima were obtained from a derivative curve; in addition, for the "b" component the peak maximum was checked by subtracting the high wavenumber half of the "a" component from the low wavenumber half and searching for a maximum in the residual counts. The two methods gave similar values for the peak positions although the "b" component had a broad maximum. The total envelope was then fitted to two Lorentz-Gaussian product functions by varying the halfwidth and peakheights to minimize the sum of the square of the residuals. Peak positions were altered slightly and the process repeated to search for smaller residuals. No attempt was made to correct for finite slitwidths but the spectrometer slitwidths were maintained at at least one quarter the Raman bandwidth. Normally this meant 0.25 cm^{-1} slits. Reasonable two-band fits which accounted for more than 95% of

the total area could be obtained with the Lorentz-Gaussian product function but attempts with pure Lorentz or pure Gaussian bandshapes were less satisfactory.

Results and Discussion

Selected portions of the Raman spectrum of a partly oriented crystal of 8% ^{18}O -enriched $\text{Sr}(\text{NO}_3)_2$ are shown in Fig. 1 and peak positions and assignments are listed in Table I for data collected at 77 and 478°K. Peak positions and depolarization ratios for the $\text{N}^{16}\text{O}_3^-$ regions were essentially identical to those previously observed for natural $\text{Sr}(\text{NO}_3)_2$ (1). In both the ν_1 and ν_4 regions additional peaks due to the $\text{N}^{18}\text{O}^{16}\text{O}_2^-$ and $\text{N}^{18}\text{O}_2^{16}\text{O}^-$ ions were observed but these did not show the correlation field coupling effects of the $\text{N}^{16}\text{O}_3^-$ peaks. Peaks at 1046 and 1036 cm^{-1} observed by Vinh *et al.* (6) and assigned to $\nu_1 - \nu_p$ (ν_p represents a

TABLE I
PEAK POSITIONS (cm^{-1}) FOR 8% ^{18}O -ENRICHED $\text{Sr}(\text{NO}_3)_2$

77°K	478°K		Species	Abundance
708.0	706		$\text{N}^{18}\text{O}_2^{16}\text{O}^-$	3.5%
714.5	712			
721.5	720		$\text{N}^{18}\text{O}^{16}\text{O}_2^-$	17%
727.5	726			ν_4
736.8	736	E_g		
738.3	737.5	F_g	$\text{N}^{16}\text{O}_3^-$	80%
741.4	739.5	F_g		
996	—		$\text{N}^{18}\text{O}_3^-$	~0.05%
	~1011	disorder	$\text{N}^{18}\text{O}_2^{16}\text{O}^-$	3.5%
1016.4	1013.6			
	1031.2	disorder	$\text{N}^{18}\text{O}^{16}\text{O}_2^-$	17%
1036.4	1033.6			ν_1
1046	1044		$\text{N}^{17}\text{O}^{16}\text{O}_2^-$	~0.6%
	1051.8	disorder		
1054.8	^a	F_g	$\text{N}^{16}\text{O}_3^-$	80%
1056.0	1054.0	A_g		
1370	1368	E_g		
1406	1403	F_g	All species	
1427	1421	F_g	contribute to ν_3	
1471	1471		$2\nu_4$	

^a Obscured.

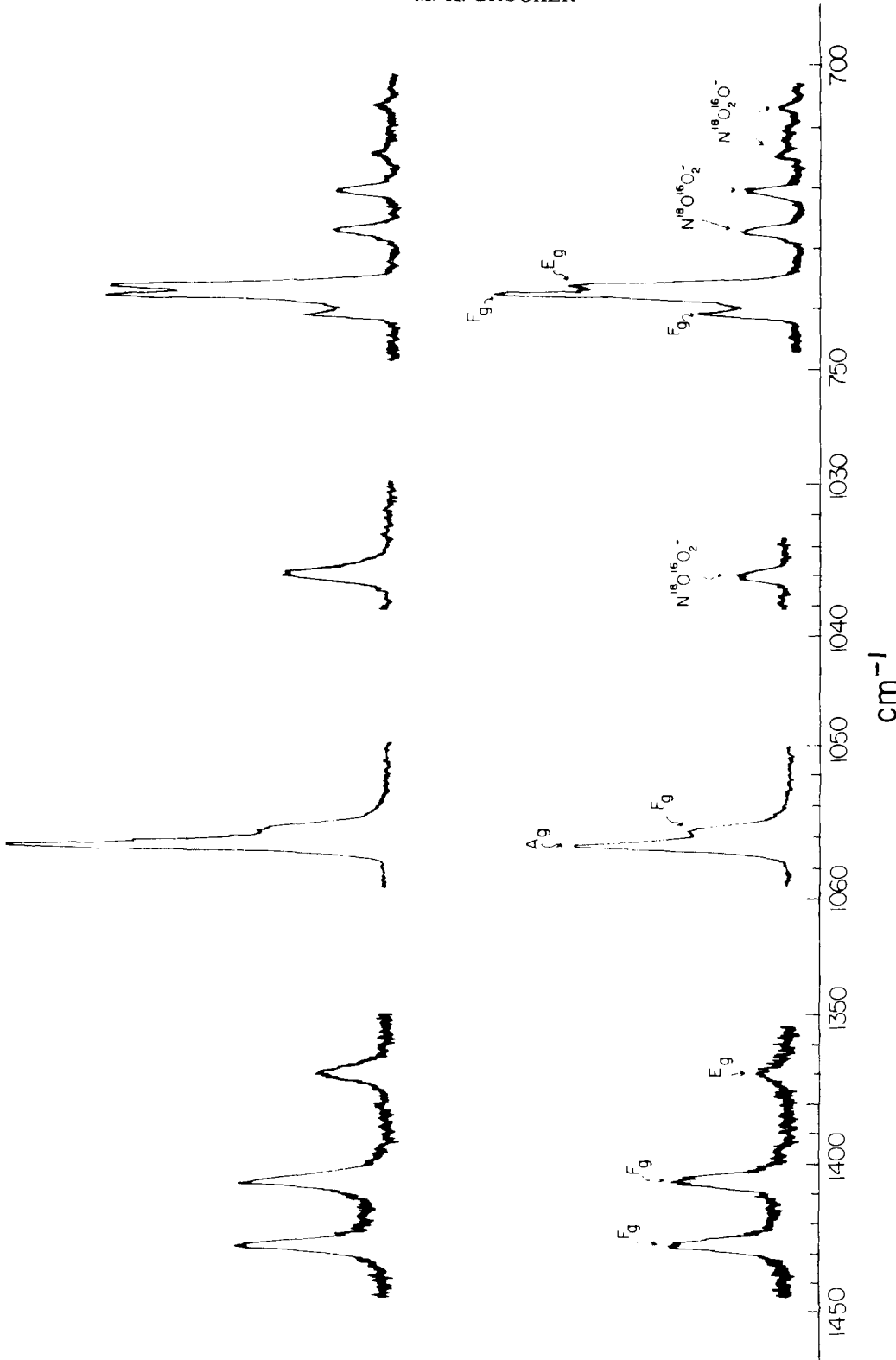


FIG. 1. Raman spectra of a partly oriented 8% ^{18}O -enriched $\text{Sr}(\text{NO}_3)_2$ crystal at 77°K. Slit widths were 0.25 cm^{-1} for 700–1060 cm^{-1} and 2.0 cm^{-1} for 1350–1450 cm^{-1} . Top: X(Y'Y)Z, Bottom: X(ZY)Z.

precession of the NO_3^- about the ternary axes) have been reassigned to the $\text{N}^{17}\text{O}^{16}\text{O}_2^-$ and $\text{N}^{18}\text{O}^{16}\text{O}_2^-$ ions. In the ν_1 region the $\text{N}^{18}\text{O}^{16}\text{O}_2^-$ and $\text{N}^{18}\text{O}_2^{16}\text{O}^-$ peaks did not show the F_g component while in the ν_4 region the three correlation field components of the $\text{N}^{16}\text{O}_3^-$ species were replaced by symmetric doublets for the $\text{N}^{18}\text{O}^{16}\text{O}_2^-$ and $\text{N}^{18}\text{O}_2^{16}\text{O}^-$ species. The symmetric doublets result from the lifting of the two-fold degeneracy of the E' mode of an isolated NO_3^- ion (D_{3h} symmetry) because ^{18}O substitution lowers the symmetry to C_{2v} (14). In the ν_3 region the three correlation field components of the $\text{N}^{16}\text{O}_3^-$ species were unperturbed by the presence of the ^{18}O containing ions but no new peaks due to these ions were detected. Similarly no new peaks were detected in the external mode region and except for a possible 1 cm^{-1} decrease of the 182 cm^{-1} mode the external region remained unaltered by the ^{18}O substitution.

The results are completely consistent with the studies of Belousov *et al.* (15) and agree with predictions that discrete local modes of isotopically substituted ions will only appear if the isotopic shift is greater than the half-width of the unshifted peak. In the ν_1 and ν_4 regions the correlation field splittings are less than 5 cm^{-1} and the halfwidths of each component less than 2 cm^{-1} , whereas the shift in peak position with ^{18}O substitution is 20 and 13 cm^{-1} per ^{18}O atom. The ν_1 and ν_4 modes of the ^{18}O substituted species therefore appear as local modes and exhibit static but not dynamic field effects. In the ν_3 region the correlation field splittings are of the order of 60 cm^{-1} with the halfwidths of each component of the order of 10 cm^{-1} , whereas the shift in peak position with ^{18}O substitution is only of the order of 6 cm^{-1} per ^{18}O atom (14). It would appear that the ^{18}O substituted species couple with the unsubstituted ions so that all ions contributed to the three correlation field components. The external mode region resembles the ν_3 region in that no local modes are observed. Again this can be attributed to the fact that

the predicted isotopic shifts of peak position are within the band halfwidth (15).

Two important facts emerge from the ^{18}O study. (a) Coupling between certain modes of the isotopically substituted impurity ions was not present even at 17% of the isotope ion; (b) the presence of 20% isotopic impurity ion did not interfere with the coupling of the host lattice.

Recent studies of a number of nitrates have indicated the existence of a weak second component in the ν_1 region at slightly lower frequency than the major component (7-11). Temperature-dependent studies have suggested that this component has either a "hot-band" (9-11) or a "disordered-site" (Frenkel type) (8, 9) origin although the distinction between the two possibilities may not be significant (9, 10). In the present study the F_g component masked this feature in the $\text{N}^{16}\text{O}_3^-$ region at room temperature but was easily detected in the $\text{N}^{18}\text{O}^{16}\text{O}_2^-$ region since the F_g mode is absent (Fig. 2, Table I). The relative intensity of the "b" component increased with increasing temperature in both regions. Above 373°K the "b" component of the $\text{N}^{16}\text{O}_3^-$ region had replaced the F_g component as the dominant feature but because of the interference from the F_g mode relative intensity measurements were performed mostly for the $\text{N}^{18}\text{O}^{16}\text{O}_2^-$ species.

Data for the effect of temperature on the band parameters of ν_1 ($\text{N}^{18}\text{O}^{16}\text{O}_2^-$) are plotted in Fig. 3. The ratio R (I_b/I_a) increases with temperature in a manner that is similar to that expected from a hot band. Tsuboi and Hisatsune (16) have measured the combination band $\nu_1 + \nu_4$ in the infrared and found that for NO_3^- in a NaCl matrix the anharmonicity constant $X_{14} = -2.8\text{ cm}^{-1}$ which is similar to the separation between the "a" and "b" components. This suggests that the "b" component could arise from NO_3^- ions in the 0001^1 excited state. However, simple Boltzmann distribution

¹ Representation for the vibrational states of the normal modes $v_{v_1} = 0, v_{v_2} = 0, v_{v_3} = 0, v_{v_4} = 1$.

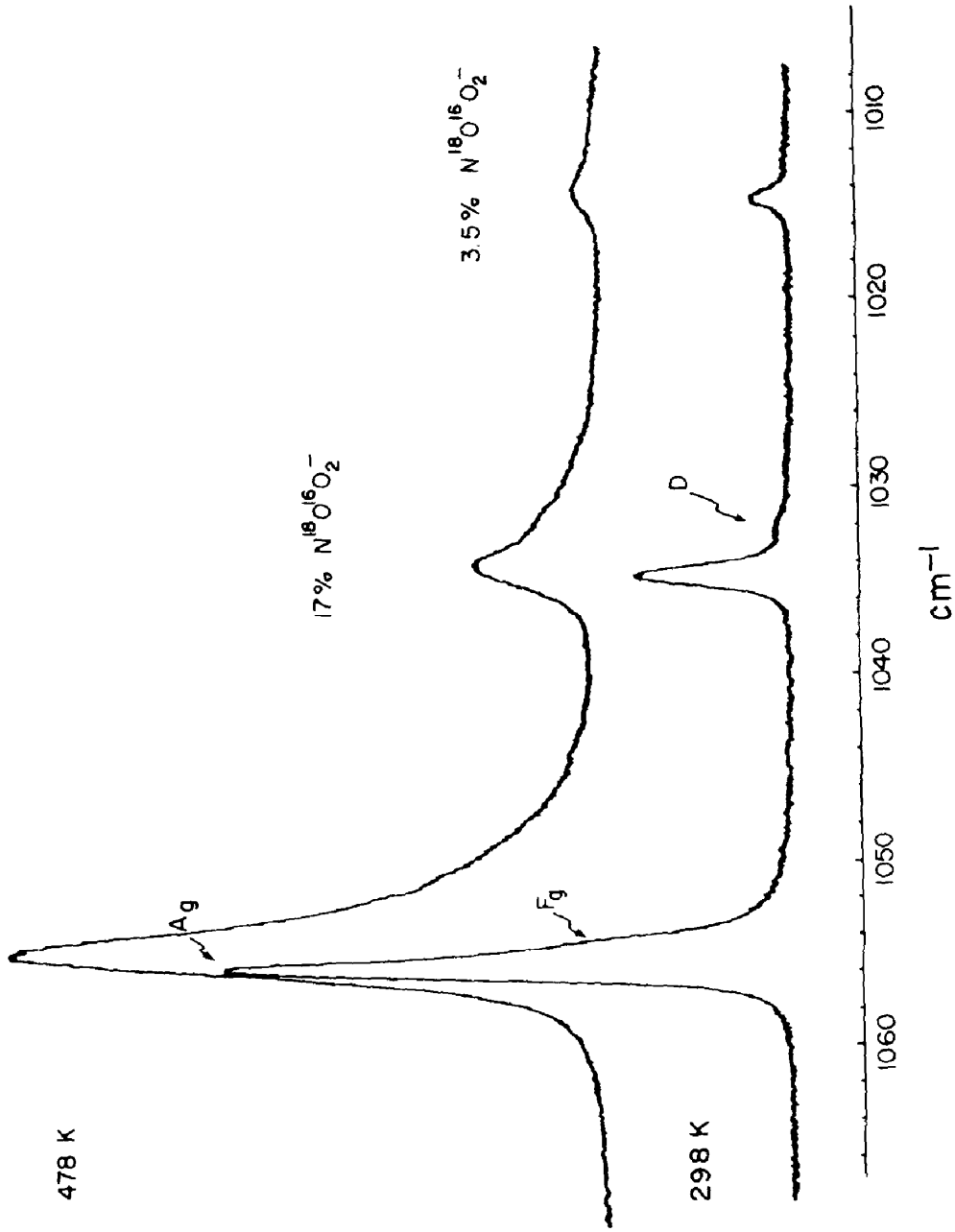


FIG. 2. Raman spectra of 8% ^{18}O -enriched $\text{Sr}(\text{NO}_3)_2$ crystal at 298 (bottom) and 478°K (top). *D* denotes anomalous disorder peak. Slit widths were 0.25 cm^{-1} .

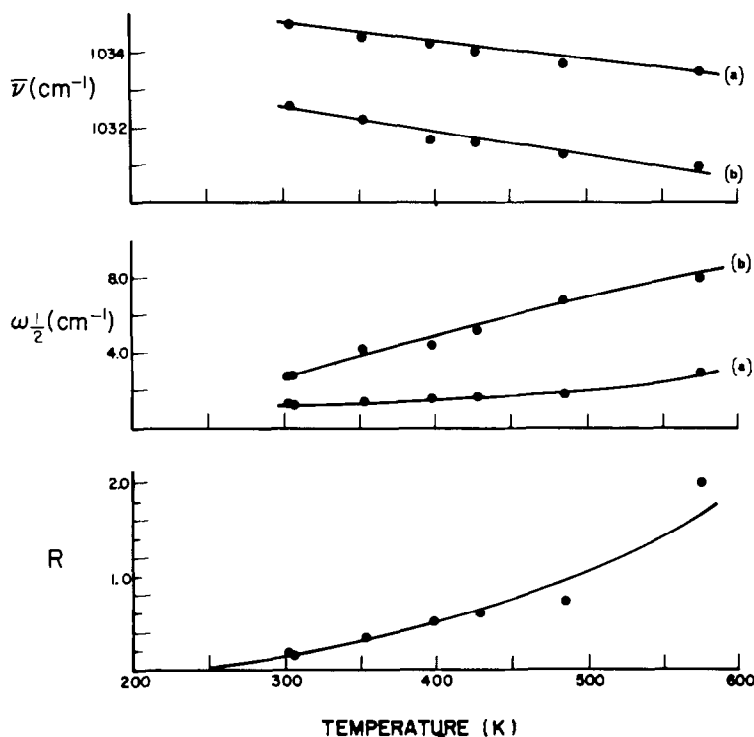


FIG. 3. Temperature dependence of the peak parameters for the "a" and "b" components of the $\text{N}^{18}\text{O}^{16}\text{O}_2^-$ ion in ^{18}O -enriched $\text{Sr}(\text{NO}_3)_2$. Top: peak positions, $\bar{\nu}$ (cm^{-1}). Middle: full width at half maximum, $\omega_{1/2}$ (cm^{-1}). Bottom: R , intensity "b" component \div intensity "a" component.

calculations for a nominal value of $\nu_4 = 740 \text{ cm}^{-1}$ give a calculated value of the intensity ratio, $R_c = 0.21$ at 490°K which is well below the measured value, $R_m = 0.7$. A contribution from 0100 with a nominal value $\nu_2 = 830 \text{ cm}^{-1}$ would increase R_c to 0.31 but the anharmonicity constant X_{12} has not been measured. Perhaps one should not expect good agreement for relative intensity ratios since many factors can lead to errors in the experimental values. Although quite reasonable analytical fits (better than 95% total area) to the observed envelope were obtained with two Lorentzian-Gaussian product functions (Fig. 4) it is possible that the solutions are not unique. The "b" component may well be a composite of a number of hot bands. From the formula for the vibrational partition function (17)

$$f_V = \prod_i (1 - e^{-1.439\bar{\nu}_i/T})^{-s_i}$$

where s_i is the degeneracy, one can estimate the populations of the various states of the vibrational manifold at 500°K ; 0000 (0.65), 0001 (0.17), 0100 (0.09), 1000 (.05), 0010 (0.04), 0002 (0.05) for nominal values of $\nu_4 = 740 \text{ cm}^{-1}$, $\nu_2 = 830 \text{ cm}^{-1}$, $\nu_1 = 1050 \text{ cm}^{-1}$ and $\nu_3 = 1380 \text{ cm}^{-1}$. Although it is most likely that the hot band would originate in ν_4 it is clear that hot bands from other states may contribute significantly. If the anharmonicity constants X_{11} , X_{12} , X_{13} , X_{14} and Y_{14} have different values a series of peaks would be expected. The fact that the "b" component is broader than the "a" component is consistent with a multiband theory. Local heating due to the laser, inadequate band shapes or slit distortion could also contribute to the large measured value of R . It does seem that external modes do not contribute since this would predict a larger value of R than observed and a

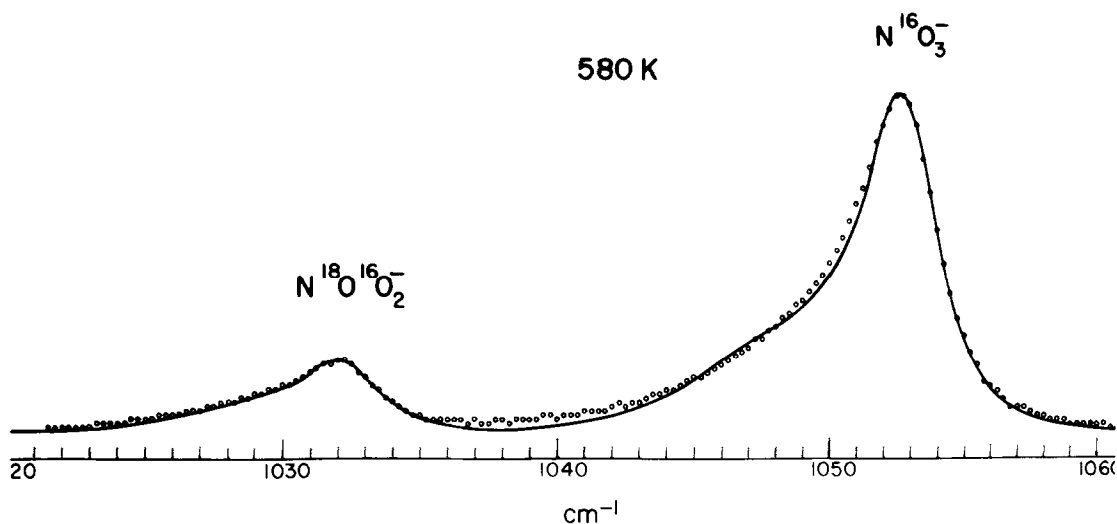


FIG. 4. Raman spectrum for 1020–1060 cm^{-1} region of ^{18}O -enriched $\text{Sr}(\text{NO}_3)_2$ at 580°K. \circ , observed points; —, calculated.

temperature dependence unlike that observed. It is also possible that sources other than simple hot bands contribute to the “*b*” component.

It would appear that vibrational modes of excited state ions can be treated as impurity modes such as the dilute ^{18}O substituted ions. In the ν_1 region at least one of the anharmonicity constants must be sufficiently large to shift the hot band by an amount greater than the halfwidth of the groundstate tran-

sition and the hot band appears as a local mode (deep center). In these and other studies we have found no evidence for additional peaks or shoulders in the ν_3, ν_4 or external mode regions which suggests that for these regions the excited state ions are coupled to the normal lattice to give a delocalized mode (shallow centre).

There have been a number of reports of low temperature phase transitions for the $\text{M}(\text{NO}_3)_2$ crystals (3–5). However, we have

TABLE II
PEAK POSITIONS FOR INTERNAL MODES OF $\text{Ca}(\text{NO}_3)_2$, $\text{Sr}(\text{NO}_3)_2$, $\text{Ba}(\text{NO}_3)_2$
AND $\text{Pb}(\text{NO}_3)_2^a$

$\text{Ca}(\text{NO}_3)_2$		$\text{Sr}(\text{NO}_3)_2$		assignment
300°K	470°K	300°K	495°K	
740.8	739	735.8	734	E_g
742.5		737.4	736	F_g
745.6	743	740.4	739	F_g
	1061.4		1052.8	(1.3, 6.6) disorder
1066.2	—	1054.4	—	F_g
1069.3	1065.0	1055.6	1054.9	(1.0, 2.0) A_g
1378	1352	1370	1366	E_g
1414		1404	1402	F_g
1425	1408	1424	1420	F_g
1483		1476	1471	$2\nu_4$

TABLE II—continued
 PEAK POSITIONS FOR INTERNAL MODES OF $\text{Ca}(\text{NO}_3)_2$, $\text{Sr}(\text{NO}_3)_2$, $\text{Ba}(\text{NO}_3)_2$
 AND $\text{Pb}(\text{NO}_3)_2^a$

$\text{Ba}(\text{NO}_3)_2$			$\text{Pb}(\text{NO}_3)_2$			assignment
300°K	480°K		300°K	485°K		
730.5	727.5		729.0	727		E_g
			731.4	729		F_g
732.0	729		734.5	731.5		F_g
	1043.1	(0.97, 7.4)		1039.4	(1.1, 10.3)	disorder
—	—		1046.5	—		F_g
1048.5	1045.6	(1.0, 2.24)	1048.5	1043.0	(1.0, 4.0)	A_g
1357	1352		1328	1316		E_g
1388	1385		1410	1420		F_g
1405	1397					F_g
1461	1457		1460	1452		$2\nu_4$

^a Room temperature data taken from Ref. 1.

^b Relative intensity, halfwidth at half height in parentheses.

found no evidence to suggest phase changes for any of strontium, barium and lead nitrate from 77 to about 525°K, the upper range of our study. Except for normal thermal broadening and the presence of the anomalous “*b*” component for ν_1 the Raman spectrum was unchanged over this temperature range (Table II, Ref. 1). Especially, the E_g and $2 F_g$ components of ν_3 and ν_4 remained even up to 525°K although beyond this temperature the resolution of the ν_4 components becomes impossible. Since first-order phase changes *have* been detected for $\text{Ca}(\text{NO}_3)_2$ at 89 and 288°K (18) it seems unlikely they would be missed for the other salts. The external mode region of $\text{Sr}(\text{NO}_3)_2$ was studied in considerable detail with an oriented single crystal in an attempt to detect anomalies similar to those reported (4–6) but no discontinuities were found in the frequency, halfwidth or intensity variations with temperature. Values of $\delta\bar{\nu}/\delta T$ and $\delta\omega_{1/2}/\delta T$ for the $\text{Sr}(\text{NO}_3)_2$ external modes over the temperature range (298–450°K) are given (Table III). They compare favorably with those reported by Vinh *et al.* (6) at lower temperature and agree with predictions by Kulkarni *et al.* (19) from lattice expansion

studies. The weak A_g mode at 61 cm^{-1} was studied carefully from 77 to 400°K since an infrared mode at this frequency was associated with suggested phase transitions at 230 and 320°K (5); however, no singularities were detected. In addition we have checked the intensity singularities reported in the 173–183°K temperature region (6). To do this the spectrometer was set at the room temperature value of the E_g mode (183 cm^{-1}) and the intensity monitored while the sample was slowly cooled to 77°K and warmed to 300°K. This was repeated at the 77°K value of the E_g mode (191 cm^{-1}) and the same process repeated for the F_g mode at 109 cm^{-1} . No anomalous intensity singularities were observed.

There are a number of anomalous observations which are more difficult to discount. Bon *et al.* (4) have reported a decrease in the thermal expansion coefficient of nearly 7% between 230 and 270°K, the same temperature region as the authors observed a break (220°K) in the curves of the infrared active lattice mode parameters. Previously Bjorseth *et al.* (3) detected low temperature anomalies ($\sim 240^\circ\text{K}$) in the dielectric constants and resistivities for strontium,

TABLE III
EFFECT OF TEMPERATURE ON PEAK PARAMETERS OF $\text{Sr}(\text{NO}_3)_2$
LATTICE MODES^a

298°K			
$\bar{\nu}$ (cm^{-1})	$\omega_{1/2}$ (cm^{-1})	$\frac{\delta\bar{\nu}}{dT}$ ($\text{cm}^{-1} \text{K}^{-1}$)	$\frac{\delta\omega_{1/2}}{\delta T}$ ($\text{cm}^{-1} \text{K}^{-1}$)
61.5	3.1	1.6×10^{-2}	0.6×10^{-2}
96	^b	—	—
109.0	4.6	2.5×10^{-2}	2.8×10^{-2}
131.5	9.5	3.5×10^{-2}	4.5×10^{-2}
165.6	11.4	3.6×10^{-2}	3.5×10^{-2}
182.5	6.8	5.5×10^{-2}	4.4×10^{-2}

^a Valid for temperature range 298–450°K.

^b Obscured due to overlap.

barium and lead nitrate. The fact that the anomalies had been observed for all ionic nitrates regardless of crystal structure prompted Bjorseth *et al.* (3) to look for a common origin and these authors suggested that a threshold in the thermal activation of modes of vibration of the nitrate group occurred near 240°K. Our measurements of the values of the intensity of the “b”

component parallels these results since we find that R approaches zero near 240°K. In Fig. 5, the calculated values of the fraction of ground state nitrate groups ($1/f_V$) have been plotted versus temperature together with measured values obtained from (I_a/I_{total}) for the ν_1 region. The resistivity, ρ_D , for $\text{Sr}(\text{NO}_3)_2$ below room temperature has been replotted on the same temperature scale

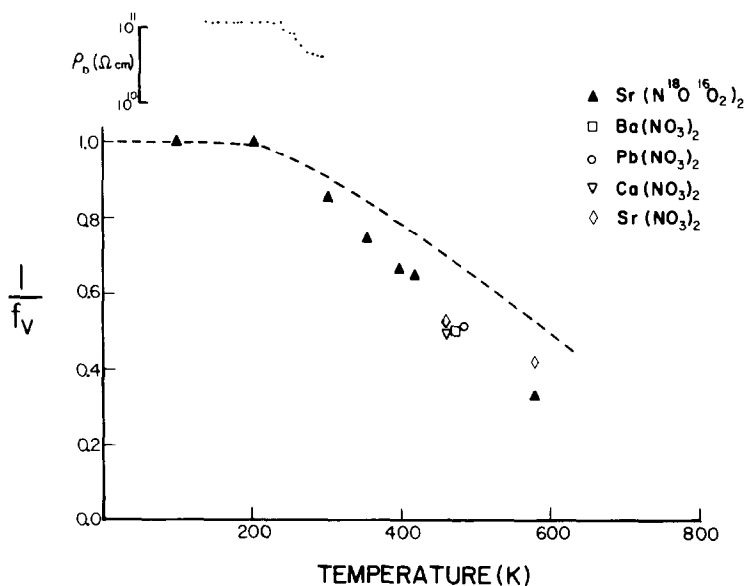


FIG. 5. Temperature dependence of the fraction of total intensity of ν_1 in the “a” component (points) compared to the Boltzmann fraction of ground state ions, $(1/f_V)$ ---. Resistivities, ρ_D , replotted from Ref. 3 are also shown plotted on the same temperature scale.

from Ref. 3 to illustrate that the resistivity reaches a constant value as the theoretical population of excited state nitrate groups approaches zero.

It would appear that the T_h^6 space group best describes the structures of $\text{Sr}(\text{NO}_3)_2$, $\text{Ba}(\text{NO}_3)_2$ and $\text{Pb}(\text{NO}_3)_2$ from 77 to $>520^\circ\text{K}$ and $\text{Ca}(\text{NO}_3)_2$ from 288 to $>520^\circ\text{K}$. Above 200°K the population of excited state nitrate groups increases (primarily in the 0001 state). These excited state ions can result in anomalous properties since they couple to the groundstate lattice in a different manner and may be treated as impurity centers. The excited state ions give rise to local modes in the ν_1 region although they are delocalized in the other internal regions and the external region. From the measured values of the intensity of the "b" component it can be seen that the host lattice (ground state groups) can tolerate a considerable number of hot ions without significant structural adjustment. It is interesting that the lattice modes which have significantly populated excited states do not give rise to local modes presumably because the anharmonicity constants are too small and transitions originating in hot external modes remain delocalized (shallow impurity centers). As is well known the lattice expansion with temperature is due to increasing populations of excited states with associated increased vibrational amplitudes (primarily in the external region). This would lead to the broadening in internal mode region. Although it is not often considered, anharmonic forces may be responsible for X-ray diffraction from Bragg reflections that are forbidden in the harmonic approximation (12). This could account for Birnstock's suggested $P2_13$ structure. It is clear that in order to understand all the properties of a crystal one needs more than the static average atomic positions provided by diffraction methods. Attempts must be made to understand the dynamic behavior and this will undoubtedly require knowledge of anharmonic terms in the force constants and

at present very little is known about these forces.

Acknowledgment

This work was supported by the National Research Council of Canada.

References

1. M. H. BROOKER AND J. B. BATES, *Spectrochim. Acta* **29A**, 439 (1973).
2. R. BIRNSTOCK, *Z. Kristallogr.* **124**, 310 (1967).
3. O. BJORSETH, J. H. FERMOR, AND A. KJEKSHUS, *Acta Chem. Scand.* **25**, 3791 (1971).
4. A. M. BON, C. BENOIT, AND J. GIORDANO, *Phys. Status Solidi. B* **78**, 453 (1976).
5. A. M. VERGNOUX AND A. M. BON, *Compt. Rend. B* **280**, 665 (1975).
6. L. D. VINH, M. ABENOZA, A. ARMENGAUD, AND J. M. PASTOR, *Spectrochim Acta* **33A**, 213 (1977).
7. YA. A.-KH. BADR, S. V. KARPOV, AND A. A. SHULTIN, *Fiz. Tverd. Tela* **15**, 2541 (1973); *Sov. Phys. Solid State*, **15**, 1692 (1974).
8. S. V. KARPOV AND A. A. SHULTIN, *Fiz. Tverd. Tela* **17**, 2868 (1975); *Sov. Phys. Solid State* **17**, 1915 (1976); *Fiz. Tverd. Tela* **18**, 730 (1976); *Sov. Phys. Solid State* **18**, 421 (1976).
9. M. H. BROOKER, *J. Chem. Phys.* **68**, 67 (1978).
10. M. H. BROOKER, *J. Phys. Chem. Solids* **39**, 657 (1978).
11. D. W. JAMES, M. T. CARRICK, AND H. F. SHURVELL, *Aust. J. Chem.* **28**, 1129 (1975).
12. B. T. M. WILLIS AND A. W. PRYOR, "Thermal Vibrations in Crystallography", Cambridge Univ. Press, 1975, p. 156.
13. A. J. MELVEGER, E. R. JOHNSON, AND E. N. LADOV, *J. Inorg. Nucl. Chem.* **32**, 337 (1970).
14. R. KATO AND J. ROLFE, *J. Chem. Phys.* **47**, 1901 (1967).
15. M. V. BELOUSOV, D. E. POGAREV, AND A. A. SHULTIN, *Phys. Status Solidi. B* **80**, 417 (1977).
16. M. TSUBOI AND I. C. HISATUNE, *J. Chem. Phys.* **57**, 2087 (1972).
17. J. C. D. BRAND AND J. C. SPEAKMAN, "Molecular Structure," p. 145, Arnold, London (1961).
18. M. H. BROOKER, *Spectrochim. Acta* **32A**, 369 (1976).
19. R. G. KULKARNI, G. K. BICHILE, M. D. KARKHANAVALA, AND A. C. MOMIN, *J. Phys. Soc. Japan* **42**, 971 (1977).